Circulation Reports
Circ Rep 2019; 1: 378–388
doi:10.1253/circrep.CR-19-0062

ORIGINAL ARTICLE
Pediatric Cardiology and Adult Congenital Heart Disease

Cardiac Function in Infants Born to Mothers With Gestational Diabetes

— Estimation of Early Diastolic Intraventricular Pressure Differences —

Satoru Iwashima, PhD; Satoshi Hayano, PhD; Yusuke Murakami, PhD; Aki Tanaka, PhD; Yumiko Joko, MD; Shuji Morikawa, MD; Mayumi Ifuku, MD; Takeshi Iso, MD; Ken Takahashi, PhD

Background: This study compared the myocardial performance of infants born to mothers with gestational diabetes mellitus (IGDM) and without GDM (controls) under the new GDM definitions.

Methods and Results: The subjects consisted of 36 IGDM and 39 control infants. GDM diagnosis was based on oral glucose tolerance test during pregnancy or the presence of diabetes prior to the current pregnancy. Between-group infant cardiac function was determined and compared using 2-D speckle tracking analysis, intraventricular pressure difference (IVPD) and IVP gradient (IVPG), using color M-mode Doppler imaging. IVPD and IVPG were higher in IGDM than in the controls, particularly the mid–apical IVPG. The global circumferential strain (GCS) and endocardial GCS were higher in IGDM than in controls. Increased maternal glycated hemoglobin was correlated with reduced transmural and epicardial GCS in the IGDM. Maternal maximum fasting blood sugar had a mild, positive correlation with IVPD and IVPG.

Conclusions: Ventricular sucking force, measured as the IVPD, IVPG, and endocardial GCS, were higher in IGDM than in the controls. A hyperglycemic environment during pregnancy leads to impaired cardiac performance in IGDM, compared with control infants. IGDM might have favorable systolic and diastolic cardiac performance due to cardiac metabolic adaptations occurring before poor glucose control causes impaired cardiac performance.

Key Words: Color M-mode Doppler imaging; Diabetic cardiomyopathy; Infant with gestational diabetes mother; Intraventricular pressure difference

Gestational diabetes mellitus (GDM) increases the risk of numerous complications in the neonate, including both structural and functional cardiovascular disease. Infants, with structurally normal hearts, born to mothers with GDM (IGDM) may develop transient myocardial hypertrophy and associated systolic and diastolic dysfunction.[1] When present, IGDM with hypertrophic cardiomyopathy (HCM) tends to spontaneously regress in the first few months of life,[2] but asymptomatic IGDM without cardiac hypertrophy develop subclinical decreases in systolic and diastolic myocardial function.[3]

Recently, new technology has been developed to estimate cardiac systolic and diastolic function, including 2-D speckle tracking echocardiography (2DST)-derived strain imaging.[4,5] Additionally, 2DST deformation imaging has superior prognostic value over conventional measures for predicting major adverse cardiac events.[6] Moreover, layer-specific myocardial strain can be measured in the endocardial, transmural, and epicardial left ventricular (LV) layers using this technique.[7] Further, intraventricular pressure differences (IVPD) and intraventricular pressure gradients (IVPG) can be measured on color M-mode imaging to accurately and non-invasively estimate active suction.[8–10] IVPD has an excellent correlation with Tau index, which is a gold standard, although Tau index is an invasive method of evaluating diastolic function.[11]

In 2010, the International Association of Diabetes and Pregnancy Study Groups recommended new criteria for the diagnosis and classification of hyperglycemia during pregnancy,[12] recognizing the increasing prevalence of undi-

Received July 11, 2019; revised manuscript received July 22, 2019; accepted July 25, 2019; J-STAGE Advance Publication released online August 28, 2019 Time for primary review: 1 day

Department of Pediatric Cardiology (S.I., S.H.), Department of Obstetrics and Gynecology (Y.M., A.T.), Department of Cardiology (Y.J., S.M.), Chutoen General Medical Center, Kakegawa; Department of Pediatrics, Juntendo University Faculty of Medicine, Tokyo (M.I., T.I., K.T.), Japan

Mailing address: Satoru Iwashima, PhD, Department of Pediatrics, Chutoen General Medical Center, 1-1 Syoubugauraike, Kakegawa 436-8555, Japan. E-mail: iwashima3617@gmail.com

ISSN-2434-0790

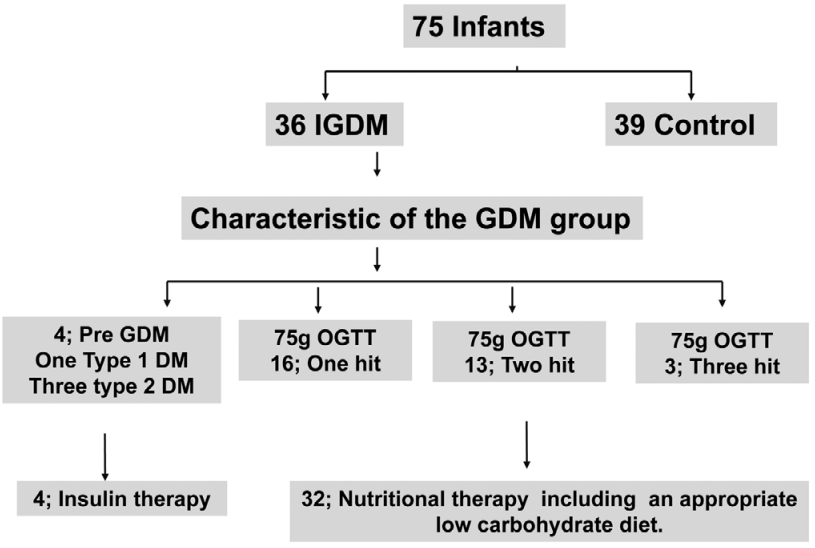

Figure 1. Study design and subject selection. DM, diabetes mellitus; GDM, gestational diabetes; IGDM, infants born to mothers with gestational diabetes; OGTT, oral glucose tolerance test.

agnosed GDM.[13] Under the new GDM definition, there is little information currently available regarding estimating myocardial changes that occur in IGDM using either conventional echocardiography or new technologies, including 2DST, IVPD, and IVPG. Thus, in this study we evaluated the myocardial performance of IGDM and control infants, using echocardiography, and assessed the factors affected by maternal glucose metabolism abnormalities under the new GDM definition.

Methods

Subjects

The subjects consisted of infants and mothers attending the Department of Pediatrics, Chutoen Medical Center, between June 2017 and October 2018. There were a total of 36 IGDM, 39 control infants, and their respective mothers. Infants were excluded if they were born at a gestational age <37 weeks, had congenital heart disease, were outside the size range for their gestational age (defined as birth weight below or above the 10th percentile for their gestational age[14]), required artificial ventilation, had Apgar score <7 at 5 min, or had chromosomal abnormalities. Mothers were excluded if they had chronic medical conditions, such as hypertension (including pregnancy-induced hypertension), gestational thyroid disease and so on. Women with GDM were defined as those with a glucose metabolism abnormality that existed prior to or began during the current pregnancy and was diagnosed on oral glucose tolerance test (OGTT). A simplified, 1-step OGTT that required only a 75-g, 2-h oral test was used.[12] Glucose metabolism abnormalities were identified on fasting blood glucose ≥92 mg/dL or blood glucose ≥180 mg/L at 1 h or ≥153 mg/dL at 2 h after consuming the glucose solution. One (one hit) or more (two and three hit) of these values from a 75-g OGTT must be equaled or exceeded for the diagnosis of GDM. **Figure 1** shows the study flow chart. In the IGDM group, 4 mothers were identified as having pre-existing type 1 (n=1) or type 2 (n=3) DM. Of the remaining 32 mothers identified with GDM following the 75-g OGTT, 16 were one hit, 13 were two hits, and 3 were three hits. The 4 mothers with type 1 or 2 DM were receiving insulin before the pregnancy and the others received nutritional counseling by a registered dietitian and were placed on appropriate, low-carbohydrate diets. Infants in the IGDM group were monitored to determine blood glucose levels after birth. When an infant's blood glucose was <40 mg/dL, an i.v. glucose infusion was given to maintain optimal glucose levels.

The Ethics Committee of Chutoen Medical Center approved the study protocol, which conformed to the principles of the Declaration of Helsinki (approval date, 21 November 2018; approval number, 85).

Data Collection

Given that this study was an observational, retrospective, historical cohort study, the results required validation using prospective evaluation in a small cohort of patients. Baseline demographic and clinical data were collected from the medical records of all participants.

Baseline Blood Pressure (BP) and Cord Blood

Replicate BP measurements were obtained from the left or right legs of relaxed, supine newborns. Infant BP was measured at the time of echocardiography. Cord blood was taken from a double-clamped cord and analyzed less than or equal to 15 min after collection.[15]

Echocardiography

A Vivid-S5 cardiac ultrasound system (GE Healthcare Japan, Tokyo, Japan) with a 6S or 12S sector array transducer was used to conduct echocardiograms when the patient was at rest. All neonates underwent routine echocardiography. The stored digital scans were analyzed by an expert blinded to patient details. Measurements from basic 2-D echocardiograms were conducted, including LV and right ventricle (RV) and atrial volume determination, using standard procedures recommended by the American Society of Echocardiography.[16] LV and RV stroke volumes and LV output were determined using pulsed Doppler imaging.[17]

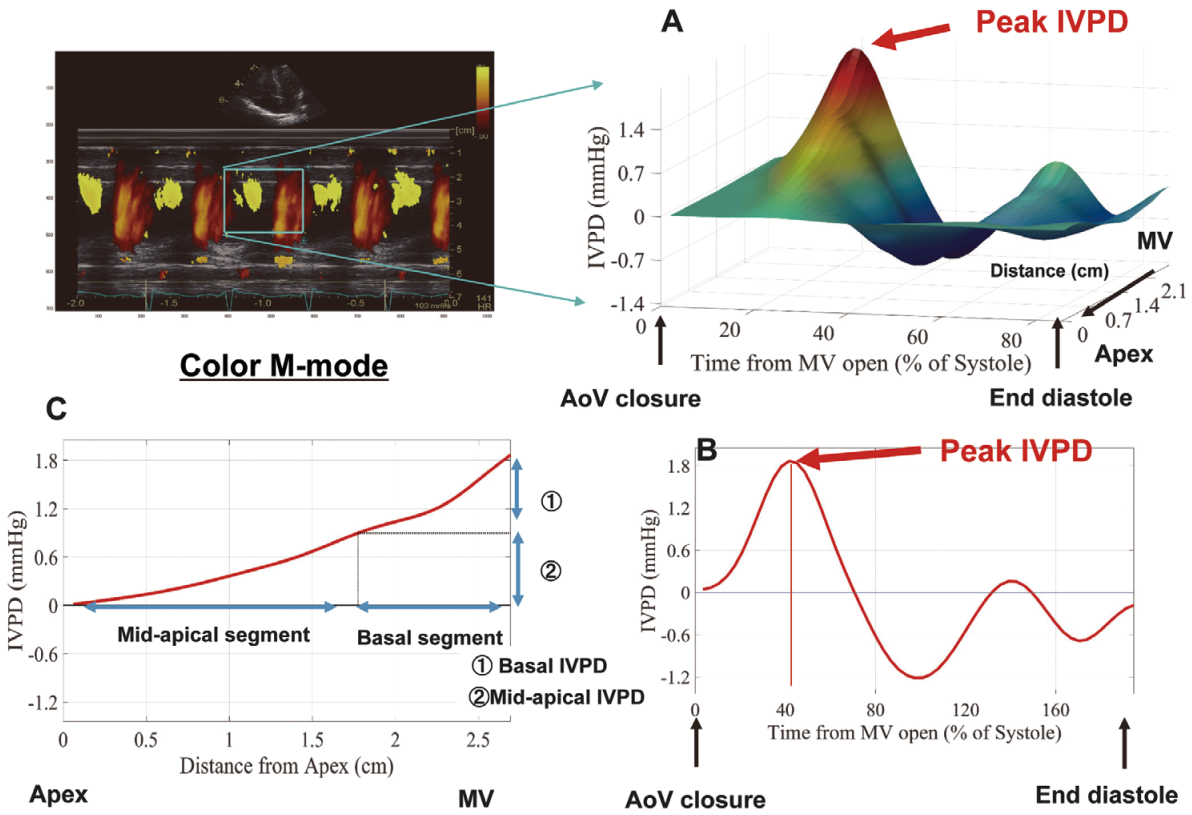

Figure 2. Estimation of early diastolic intraventricular pressure difference (IVPD). (**A**) Three-dimensional temporal and spatial profiles of IVPD. (**B**) Temporal profile at peak total IVPD and mid-apical IVPD. (**C**) IVPD spatial profile at peak IVPD, at the MV level. The basal and mid-apical IVPD segments were calculated based on the left ventricle segmentation rule of one-third for basal and two-thirds for mid-apical. AoV, aortic valve; MV, mitral valve.

IVPD and IVPG

IVPD was estimated using color M-mode imaging to integrate the 1-D Euler equation, as previously described.[18] The images were obtained using the same apical 4-chamber view that was used to assess LV ejection fraction and mitral motion (**Figure 2**). The flow velocity color M-mode images were acquired by aligning the Doppler cursor in parallel with the diastolic inflow and were analyzed using MATLAB (MathWorks, Natick, MA, USA) and an image processing algorithm. This method was previously validated against direct micromanometer measurements.[19,20] The peak IVPD from the mitral valvular annulus to the LV apex was calculated using the temporal profile of the LV apex pressure relative to the left atrial (LA) pressure. Peak IVPD and the timing of the peak IVPD from the onset of the Q-wave were measured from at least 3 beats; the mean was used in the final analysis.

The total IVPD was further separated into the basal and mid and apical segments (hereafter, basal and apical segments), as previously described (**Figure 2**).[8] Furthermore, to overcome differences in LV size, we calculated the IVPG as IVPD/LV length.[8–10,21] The basal segment was defined as one-third of the total LV length from the mitral valve, whereas the apical segment was defined as the remaining two-thirds. The timing of Q-wave onset, aortic valve closure, and mitral valve opening were measured using Pulse Doppler Wave imaging. To overcome heart rate differences, the timings of all parameters were normalized to the duration of systole (i.e., at the onset of the QRS-wave [t=0%] and at end-systole [t=100%]).[22] Experts, blinded to the patient details, analyzed the stored digital scans.

Myocardial Layer-Specific Strain on 2DST

The 2DST analyses were retrospectively performed using vendor-specific software (EchoPAC PC, version 201, GE Healthcare) by an experienced observer, blinded to patient information. Manual tracings of the endocardial border during end-systole, in 3 apical views and at 3 levels of the short axis views, were performed to measure longitudinal and circumferential strain. The software performed speckle tracking over the entire myocardium included in the region of interest, allowing assessment of the relationship between layer-specific strain parameters and fundamental anthropometric variables. Subsequently, the software determined strain and strain rate at the transmural (not midwall) and endocardial locations, epicardial strain, the ratio of endocardial longitudinal (circumferential) strain at end-systole (GL(C)S) to epicardial GL(C)S, diastolic global longitudinal peak strain rate–early (DGLSR e), DGLSR–late (DGLSR a), DGLSR e/a ratio, diastolic global circumferential peak strain rate–early (DGCSR e), DGCSR–late (DGCSR a), and DGCSR e/a ratio. This recently introduced speckle-

Table 1. Subject Characteristics (n=75)

	IGDM group (n=36)	Control group (n=39)	P-value
Sex (male)	18 (50.0)	17 (43.6)	0.647
GA (weeks)	39 (38~39)	39 (38~40)	0.187
Apgar score (5-min)	9 (9~9)	9 (9~9)	0.138
Length (cm)	50.5 (50.0~51.0)	50.0 (49.0~51.0)	0.108
Weight (g)	3,175 (2,892~3,464)	2,948 (2,838~3,223)	0.039
BSA (m^2)	0.21 (0.20~0.22)	0.21 (0.20~0.21)	0.038
Time to echo (days)	1 (1~1)	1 (1~2)	0.06
Cardiac variables			
HR (beats/min)	125 (114~136)	120 (107~130)	0.217
SBP (mmHg)	67 (60~67)	65 (59~71)	0.668
DBP (mmHg)	38 (35~43)	36 (31~38)	0.041
MBP (mmHg)	49 (45~54)	48 (43~53)	0.352
M-mode parameters			
LVDd (mm)	17.3 (16.3~18.5)	18 (17.0~19.1)	0.353
LVDs (mm)	11.3 (10.9~12.4)	11.5 (10.9~12.3)	0.545
IVSd (mm)	3.6 (3.3~4.2)	3.3 (2.7~3.6)	0.003
IVSs (mm)	3.9 (3.4~4.4)	3.7 (3.3~3.9)	0.102
LVPWd (mm)	2.5 (2.3~2.7)	2.6 (2.4~2.8)	0.615
LVPWs (mm)	3.8 (3.5~4.2)	3.7 (3.3~3.9)	0.093
LVEF (%)	69.5 (66.5~73.8)	71.9 (69.1~74.7)	0.154

Data given as n (%) or median (IQR). BSA, body surface area; DBP, diastolic blood pressure; GA, gestational age; HR, heart rate; IGDM, infants with structurally normal hearts, born to mothers with gestational diabetes mellitus; IVSd, intraventricular septal wall thickness at diastole; IVSs, intraventricular septal wall thickness at systole; LVDd, left ventricular diastolic dimension; LVDs, left ventricular systolic dimension; LVEF, left ventricular ejection fraction; LVPWd, left ventricular posterior wall thickness at diastole; LVPWs, left ventricular posterior wall thickness at systole; MBP, mean blood pressure; SBP, systolic blood pressure.

tracking echocardiography technology allows non-invasive bedside assessment of layer-specific myocardial deformations.[7,23] We used a 2DST analysis that incorporated a high sampling rate (median, 78 samples/s; range, 66–137 samples/s). An expert, blinded to patient details, analyzed the stored digital scans. This new, sensitive indicator is highly effective in detecting cardiac dysfunction in various cardiac diseases, including in children.[24–27]

Outcomes

The primary outcomes were comparisons of the myocardial performance of IGDM and control infants on conventional 2-D echocardiography, 2DST, IVPD, and IVPG. The secondary outcome was identification of the factors affecting myocardial performance in IGDM. We also investigated the relationships between echocardiography parameters, IVPD, and IVPG, and maternal factors.

Measurement Reproducibility

To reduce recall bias, intra- and interobserver variability in the measurement of 2-D global strain; the strain rate of the transmural myocardium, endocardium, and epicardium; and diastolic global strain rate in both the longitudinal and circumferential directions were recorded in 10 randomly selected infants by 2 independent observers and by one of the observers on 2 different occasions. IVPD and IVPG measurement on color M-mode imaging has been previously shown to be accurate and reproducible.[18]

Statistical Analysis

The results are expressed as median (IQR). Two-sided comparisons between the control and IGDM groups were performed using the Mann-Whitney U-test, chi-squared test, or Fisher's exact test, as appropriate. Spearman's rank correlation was used to evaluate the relationship between echocardiographic and other findings. Comparisons involving more than 3 variables were tested using the Kruskal-Wallis test. Post-hoc analyses were performed using the Bonferroni test. The variables found to be significant on univariate analysis were assessed on multivariate analysis using stepwise logistic regression. Observer variability parameters were used to calculate mean bias (average difference between measurements), SD, 95% CI, coefficients of variation using the Bland-Altman approach, and the intra-class correlation coefficient. For all statistical analysis, performed using SPSS Statistics 21 (SPSS, Chicago, IL, USA), $P<0.05$ was considered significant.

Results

Primary Outcome

A comparison of the baseline characteristics and echocardiography parameters of IGDM and controls are shown in **Table 1** and **Supplementary Table 1**. On conventional echocardiography, the median intraventricular septal wall thickness at diastole (IVSd) was greater in the IGDM group than in the control group. The between-group comparison of color M-mode and 2DST analyses are shown in **Table 2**. On univariate analysis of the color M-mode data, total IVPD, apical IVPD, and IVPG were higher in the IGDM group than in the control group. Specific-layer GLS analyses failed to show any significant differences between the

Table 2. 2-D Speckle Tracking and Color M-Mode Analysis

	IGDM group (n=36)	Control group (n=39)	P-value
GLS			
Global (%)			
Transmural GLS	−13.4 (−14.4~−11.9)	−12.9 (−14.1~−11.0)	0.201
Endocardial GLS	−16.6 (−18.6~−14.8)	−16.4 (−17.1~−13.4)	0.234
Epicardial GLS	−10.9 (−12.2~−9.6)	−10.6 (−11.9~−9.1)	0.442
GLS Endo/Epi ratio	1.51 (1.43~1.60)	1.48 (1.40~1.57)	0.228
DGLSR (s^{-1})			
DGLSR e	1.9 (1.4~2.5)	1.3 (1.1~1.0)	0.003
DGLSR a	1.1 (0.8~1.4)	0.9 (0.7~1.2)	0.067
DGLSR e/a ratio	1.8 (1.2~2.6)	1.6 (1.1~2.0)	0.381
GCS			
Base (%)			
Transmural GCS	−10.3 (−12.0~−8.6)	−8.8 (−10.8~−7.2)	0.094
Endocardial GCS	−21.0 (−23.5~−17.0)	−17.0 (−21.1~−14.7)	0.016
Epicardial GCS	−4.8 (−7.3~−3.4)	−4.6 (−7.0~−3.4)	0.679
GCS Endo/Epi ratio	3.10 (2.73–4.43)	3.23 (2.44–4.68)	0.577
Middle (%)			
Transmural GCS	−12.8 (−14.4~−10.5)	−11.3 (−13.6~−9.6)	0.193
Endocardial GCS	−24.5 (−28.1~−20.4)	−21 (−23.9~−18.6)	0.017
Epicardial GCS	−5.6 (−6.7~−5.1)	−6.4 (−8.5~−4.9)	0.319
GCS Endo/Epi ratio	3.88 (3.51~4.65)	3.08 (2.56~3.80)	0.008
DGCRS e	1.4 (1.2~1.6)	1.2 (0.9~1.5)	0.086
DGCRS a	0.7 (0.6~0.9)	0.6 (0.5~0.8)	0.121
DGCRS e/a	1.9 (1.4~2.6)	2.0 (1.2~2.7)	0.866
Apex (%)			
Transmural GCS	−16.9 (−18.9~−14.1)	−16 (−17.7~−14.0)	0.256
Endocardial GCS	−33.6 (−37.3~−29.5)	−30 (−31.9~−26.2)	0.014
Epicardial GCS	−8 (−9.5~−5.8)	−7.1 (−9.3~−5.5)	0.519
GCS Endo/Epi ratio	4.38 (3.19~5.60)	3.77 (3.21~4.82)	0.467
DGCRS (s^{-1})			
Base			
DGCSR e	1.0 (0.8~1.3)	0.8 (0.7~1.1)	0.149
DGCSR a	0.6 (0.5~0.8)	0.6 (0.4~0.8)	0.379
DGCSR e/a ratio	1.6 (1.2~2.3)	1.4 (1.1~2.1)	0.618
Middle			
DGCRS e	1.4 (1.2~1.6)	1.2 (0.9~1.5)	0.086
DGCRS a	0.7 (0.6~0.9)	0.6 (0.5~0.8)	0.121
DGCRS e/a ratio	1.9 (1.4~2.6)	2.0 (1.2~2.7)	0.866
Apex			
DGCRS e	1.7 (1.6~2.0)	1.6 (1.2~1.9)	0.144
DGCRS a	0.8 (0.7~1.2)	0.7 (0.6~1.0)	0.303
DGCRS e/a ratio	1.9 (1.4~2.6)	1.8 (1.6~2.8)	0.965
Color M-mode			
Total IVPD (mmHg)	1.05 (0.90~1.25)	0.85 (0.70~0.97)	0.001
Basal IVPD (mmHg)	0.53 (0.41~0.65)	0.51 (0.37~0.57)	0.252
Mid-apical IVPD (mmHg)	0.50 (0.38~0.56)	0.35 (0.27~0.41)	<0.001
Total IVPG (mmHg/cm)	0.38 (0.32~0.44)	0.29 (0.24~0.35)	0.003
Basal IVPG (mmHg/cm)	0.23 (0.17~0.28)	0.21 (0.16~0.25)	0.308
Mid-apical IVPG (mmHg/cm)	0.21 (0.17~0.24)	0.15 (0.11~0.18)	<0.001

Data given as median (IQR). DGCSR, diastolic global circumferential strain rate; DGCSR a, DGCSR late peak strain rate; DGCSR e, DGCSR early peak strain rate; DGLSR, diastolic global longitudinal strain rate; DGLSR a, DGLSR late peak strain rate; DGLSR e, DGLSR early peak strain rate; GCS, global circumferential strain; GLS, global longitudinal strain; IGDM, infants with structurally normal hearts, born to mothers with gestational diabetes mellitus; IVPD, intraventricular pressure difference; IVPG, intraventricular pressure gradient.

Table 3. Multiple Regression Analysis (Stepwise)

	IGDM group (n=36)	Control group (n=39)	P-value	
			Univariate	Multivariate
DBP (mmHg)	38 (35~44)	36 (31~38)	0.023	
IVSd (mm)	3.6 (3.3~4.2)	3.3 (2.7~3.6)	0.003	0.010
DGLSR e	1.9 (1.4~2.5)	1.3 (1.1~1.0)	0.003	
Base GCS endocardial	−21.0 (−23.5~−17.0)	−17.0 (−21.1~−14.7)	0.016	
Middle GCS Endocardial	−24.5 (−28.1~−20.4)	−21 (−23.9~−18.6)	0.017	
Middle GCS Endo/Epi ratio	3.88 (3.51~4.65)	3.08 (2.56~3.80)	0.008	
Apex GCS Endocardial	−33.6 (−37.3~−29.5)	−30 (−31.9~−26.2)	0.014	
Total IVPD (mmHg)	1.05 (0.90~1.25)	0.85 (0.70~0.97)	0.001	0.0008
Mid-Apical IVPD (mmHg)	0.50 (0.38~0.56)	0.35 (0.27~0.41)	<0.001	
Total IVPG (mmHg/cm)	0.38 (0.32~0.44)	0.29 (0.24~0.35)	0.003	
Mid-Apical IVPG (mmHg/cm)	0.21 (0.17~0.24)	0.15 (0.11~0.18)	<0.001	

Data given as median (IQR). GLSR e, global longitudinal strain rate early peak strain rate. Other abbreviations as in Tables 1,2.

groups. On specific-layer analysis of the GCS, endocardial GCS at the basal and apical levels was higher in the IGDM group than in the controls. Further, the GCS endocardial/epicardial ratio at the middle level was also higher in the IGDM group than in the controls. On stepwise multiple linear regression analysis (**Table 3**) using dependent variables that were significant on univariate analysis, significant between-group differences were observed for IVSd and apical IVPG (R^2=0.334; IVSd: β=0.406, P=0.003; apical IVPG: β=0.355, P=0.008).

Secondary Outcomes

The maternal baseline (pregnancy) characteristics were compared between the IGDM and control infants (**Supplementary Table 2**). On univariate analysis significant between-group differences were seen in age, weight gain during pregnancy, and maximum fasting blood sugar during pregnancy. The cord blood samples also showed significant between-group differences in carbon dioxide partial pressure and potassium concentration.

On comparison of conventional echocardiography, 2DST, and color M-mode parameters between women taking insulin and those managing their diabetes with nutritional therapy, there was no significant differences. The relationship between maternal hemoglobin A1c (HbA1c) and infant myocardial performance is shown in **Figure 3**. Maternal HbA1c had a positive correlation with transmural GCS (r=0.441, P<0.05), epicardial GCS (r=0.598, P=0.01), and endocardial/epicardial GCS ratio (r=0.503, P<0.05) at the basal level. HbA1c did not correlate with endocardial data (r=0.182) data and was negatively correlated with the endocardial/epicardial GCS ratio at the apex level (r=0.472, P<0.05). There was no significant correlation between HbA1c and GLS in the specific layers and color M-mode parameters.

Other Outcomes

The correlations of IVPD and IVPG with maternal factors, M-mode, Doppler, tissue Doppler image (TDI), and 2DST parameters are listed in **Supplementary Table 3**. Maternal maximum fasting blood sugar had a mild positive correlation with IVPD and IVPG. The mitral E wave and IVS-TDI E' had a mild positive correlation with IVPD and IVPG. Myocardial layer-specific strain testing, using 2DST, showed that GLS had a weak–mild negative correlation with IVPD and IVPG. Similarly, DGLSR e show a mildly positive correlation with IVPD and IVPG. Endocardial and transmural GCS at the base and middle of the ventricle showed weakly to mildly negative correlations with IVPD and IVPG. The layer-specific DGCSR e for the 3 areas of the ventricle had weak–mild positive correlations with IVPD and IVPG.

Reproducibility

The intra- and interobserver variability scores for layer-specific 2DST and GLS and GCS diastolic myocardial strain rate were within an acceptable range (**Table 4**).

Discussion

Cardiac Performance: IGDM vs. Control

In the present study, IVPD and IVPG were higher in the IGDM group than in the control group, especially for apical IVPG. One 2DST analysis, there were no significant between-group GLS differences for any of the myocardial layers. In contrast, endocardial GCS was significantly higher at all levels in the IGDM group than in the controls. In previous cardiac performance studies involving IGDM infants, impaired LV systolic and diastolic function was seen in infants with and without cardiac hypertrophy, following poor glycemic control during pregnancy.[1,28,29] In the present study, however, favorable systolic and diastolic performance was seen in the IGDM, compared with control infants. This apparent discrepancy may be explained by other previously published studies. In a previous experimental study the LV peak filling rate on magnetic resonance imaging was significantly higher in diabetic mice than in non-diabetic mice with heart failure induced by pressure overload.[30] In addition, other previous studies have investigated favorable systolic performance in conditions of increased afterload, monitored using strain-imaging techniques. It was shown that the GLS was uniformly lower in individuals with diabetes than in controls,[31,32] whereas the GCS changes were variable.[33–38] Although GLS is known to be reduced in IGDM,[39] GCS has not been elucidated in this population. GCS mechanics may be viewed as the "myocardial compensatory domain", especially in increased afterload situations, such as hyperten-

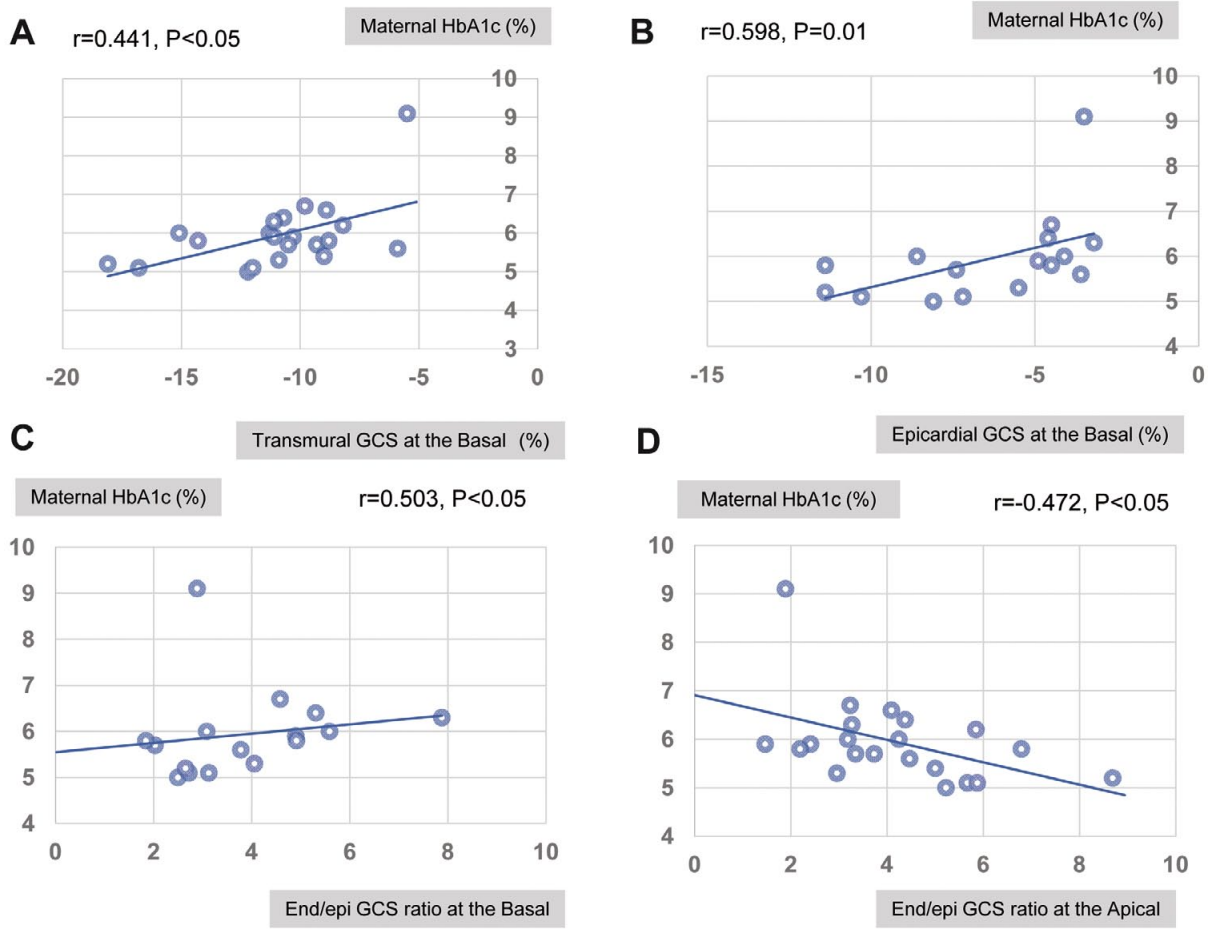

Figure 3. Correlation between maternal glycated hemoglobin (HbA1c) and infant myocardial performance. Maternal HbA1c correlated positively with (**A**) transmural global circumferential strain (GCS), (**B**) epicardial GCS, and (**C**) endo/epi GCS ratio at base levels but not with the endocardial GCS (r=0.182). (**D**) HbA1 is negatively correlated with endocardial/epicardial GCS ratio at the apex level.

sion, obstructive HCM, and severe aortic stenosis.[33,40–42] We speculate that GCS in IGDM is maintained or increased during GLS reductions due to hyperinsulinemia and overall poor glycemic control during pregnancy.

The mechanism associated with the favorable systolic and diastolic performances in IGDM is suggested to involve metabolic adaptations in the heart. In diabetic mice, these adaptations seem to prevent the heart from failing during conditions of pressure overload, suggesting that a restoration of the balance between glucose and fatty acid (FA) utilization is beneficial for cardiac function.[30] Further, metabolic remodeling of the heart may be an important contributor to the development of heart failure.[43] The transition to heart failure is generally accepted to be accompanied by a shift in cardiac substrate preference, with a greater reliance on glucose utilization and a concomitant suppression of FA oxidation (FAO).[44–46] This metabolic shift seems to precede the onset of cardiac dysfunction.[47] The diabetic heart appears to rely almost exclusively on FAO and has lost the flexibility to switch from FAO to glucose utilization.[48] Unfortunately, the nearly total reliance on FAO may be detrimental to the diabetic heart; a shift from FAO to glucose utilization, in heart failure, may be a beneficial adaptation. At birth, the rapid changes in pre- and afterloading that occur due to the fall in pulmonary vascular resistance and clamping of the cord, may result in occult myocardial injury. These echocardiography findings are consistent with changes in cardiac biomarkers, including serum cardiac troponin T and B-type natriuretic peptide, which increase from birth through the first day of life.[49–51]

Moreover, a hyperglycemic environment during pregnancy may impair cardiac performance in IGDM, but favorable glycemic control during pregnancy can prevent harmful cardiac effects. This leads to the speculation that metabolic adaptations occur in the heart to restore the balance between glucose and FA utilization in IGDM.

IGDM Cardiac Performance and Maternal Glucose Metabolism Abnormalities

Increased maternal HbA1c was associated with reduced transmural and epicardial GCS and increased endocardial/epicardial GCS ratios at the base of the ventricle, and with decreased endocardial/epicardial GCS ratios at the apex. There was no significant correlation between HbA1c and

Table 4. Intra- and Inter-Observer Variability in Layer-Specific GSR and Diastolic MSR

	Bias	SD	95% CI		CV	ICC	95% CI	
GLS								
Intra-observer variability								
Transmural	1.153	1.039	−0.546	1.831	0.90	0.735	0.349	0.910
Endocardial	1.602	1.167	−0.973	2.600	0.73	0.893	0.698	0.966
Epicardial	1.576	1.417	1.576	1.417	0.90	0.524	0.008	0.824
DGLSR e	−0.335	0.450	−0.335	0.450	1.34	0.480	−0.052	0.804
DGLSR a	−0.095	0.127	−0.095	0.127	1.34	0.881	0.668	0.962
Inter-observer variability								
Transmural	0.642	1.769	−0.546	1.831	2.76	0.941	0.780	0.984
Endocardial	0.814	2.659	−0.973	2.600	3.27	0.843	0.418	0.958
Epicardial	0.714	1.682	−0.416	1.845	2.36	0.928	0.734	0.981
DGLSR e	−0.066	0.230	−0.221	0.089	3.48	0.951	0.817	0.987
DGLSR a	0.033	0.271	−0.150	0.215	8.21	0.768	0.139	0.938
GCS								
Intra-observer variability								
Base								
Transmural	0.223	1.277	−0.549	0.995	5.73	0.926	0.783	0.976
Endocardial	0.754	1.038	0.127	1.381	1.38	0.967	0.901	0.990
Epicardial	−0.617	0.802	−1.126	−0.107	1.30	0.941	0.816	0.982
DGCSR e	0.131	0.278	−0.037	0.299	2.13	0.629	0.164	0.869
DGCSR a	0.056	0.164	−0.044	0.155	2.96	0.868	0.636	0.957
Middle								
Transmural	0.233	1.005	−0.405	0.872	4.31	0.941	0.817	0.983
Endocardial	−0.383	1.946	−1.620	0.853	5.08	0.943	0.821	0.983
Epicardial	0.325	0.422	0.057	0.593	1.30	0.928	0.780	0.978
DGCSR e	−0.083	0.185	−0.201	0.034	2.22	0.869	0.622	0.960
DGCSR a	0.027	0.174	−0.084	0.137	6.47	0.878	0.645	0.963
Apex								
Transmural	−0.592	2.109	−1.867	0.682	3.56	0.814	0.511	0.939
Endocardial	0.554	2.082	−0.704	1.812	3.76	0.876	0.656	0.960
Epicardial	−0.438	0.922	−0.996	0.119	2.10	0.958	0.874	0.987
DGCSR e	0.246	0.304	0.062	0.430	1.24	0.753	0.385	0.917
DGCSR a	−0.054	0.282	−0.224	0.116	5.23	0.696	0.277	0.895
Inter-observer variability								
Base								
Transmural	1.360	1.503	0.440	0.781	1.10	0.959	0.833	0.990
Endocardial	2.090	1.120	1.289	2.891	0.54	0.992	0.966	0.998
Epicardial	0.440	0.781	−0.118	0.998	1.77	0.982	0.927	0.996
DGCSR e	−0.140	0.217	−0.295	0.015	1.55	0.940	0.760	0.985
DGCSR a	−0.040	0.143	−0.142	0.062	3.57	0.964	0.856	0.991
Middle								
Transmural	0.480	1.470	−0.572	1.532	3.06	0.962	0.846	0.991
Endocardial	0.240	1.755	−1.02	1.50	7.31	0.971	0.884	0.993
Epicardial	0.480	1.002	−0.237	1.197	2.09	0.983	0.930	0.996
DGCSR e	0.060	0.084	0.000	0.120	1.41	0.984	0.934	0.996
DGCSR a	−0.070	0.125	−0.239	0.059	2.31	0.867	0.465	0.967
Apex								
Transmural	−0.755	1.495	−1.759	0.250	1.98	0.960	0.851	0.989
Endocardial	−0.764	1.660	−1.879	0.351	2.17	0.979	0.921	0.994
Epicardial	−0.155	1.140	−0.921	0.612	7.35	0.962	0.858	0.990
DGCSR e	0.049	0.178	−0.071	0.168	3.63	0.970	0.889	0.992
DGCSR a	0.036	0.175	−0.081	0.154	4.86	0.902	0.634	0.974

CV, coefficient of variation; GSR, global strain rate; ICC, intra-class correlation coefficient; MSR, myocardial strain rate. Other abbreviations as in Tables 1,2.

GLS in any of the myocardial layers. Cardiac hypertrophy in IGDM may be caused by fetal hyperinsulinemia, which increases the synthesis and deposition of fat and glycogen in myocardial cells.[52] In patients with HCM, reductions in specific-layer GLS and in transmural and epicardial GCS were observed to impair myocardial function, but the preserved endocardial GCS might reflect the effect of compensation for the impaired myocardial function through an increase in relative wall thickness.[53] In the present study, GLS in IGDM were different but GCS were similar to adult HCM models; there might be a pathogenic difference between adults with HCM and IGDM with HCM.[54] Even in normal individuals, GCS is known to have a transmural gradient, with lower GCS in the epicardial layers and higher values in the endocardial layers.[7] Hence, we speculate that elevated maternal HbA1c is initially harmful to transmural and epicardial GCS. The reasons for the different results in the relationship between maternal HbA1c and the endocardial/epicardial GCS ratios at the ventricle base and apex are unclear. There might be other differences, however, between the base and apex, such as in the extent of cardiac remodeling, wall thickness and so on. Further study is needed to explain the observed relationship between maternal HbA1c and the endocardial/epicardial GCS ratio.

The correlations between maternal maximum fasting blood sugar and IVPD and IVPG might also be explained by metabolic adaptations in the heart, as described here.

IVPD, IVPG, and Other Parameters

On echocardiography the diastolic parameters, including mitral E wave, IVS-TDI, E′, and DGCSR e, had mild positive correlations with IVD and IVPG. In contrast, the systolic parameters, including layer-specific GLS and base and transmural GCS, had weak–mild negative correlations with IVPD and IVPG. These results are similar to those previously reported in adults.[55] Elucidating the causal relationships between LV wall mechanics and IVPD and IVPG is difficult because they occur almost simultaneously and interact with each other. Further study is therefore needed to clarify these relationships.

Present Study and Past Studies

The present study investigated diastolic performance on color M-mode echocardiography whereas conventional methods for assessing diastolic performance using echocardiography involve mitral E and A wave measurements and TDI. These conventional methods have limitations due to their dependence on loading conditions and their limited accuracy in patients with regional myocardial dysfunction.[56] The suction force, during early diastole, from the LA to the LV apex has been thought to play an important role in diastolic function, with apical IVPD being important for the creation of active suction.[9,10,20,21,55–58] Additionally, the present definition of GDM involved the new guideline recommendations, and the mothers with GDM, in the present study, mostly had HbA1C in the normal range, had favorable weight control, and exercised favorable glycemic control throughout their pregnancies.

Study Limitations

This study has several limitations. First, this study involved a relatively small number of patients and used a retrospective design. Second, the high frame rate required for 2DST[59] may have meant that the 2DST measurements were underestimated due to the high neonatal heart rates. Third, there were a few mothers in the GDM group who were being treated with insulin, possibly introducing bias. Despite these limitations, this study provides some significant new insights. Additional studies, involving larger numbers of individuals, are needed to confirm the observed correlations.

Conclusions

Favorable systolic and diastolic performance was seen in IGDM whose mothers maintained favorable glycemic control during pregnancy. This suggests that cardiac metabolic adaptations restore the balance between glucose utilization and FAO to prevent harmful myocardial effects due to maternal GDM.

Acknowledgments

The authors thank Ryosuke Shiozawa, Soichiro Yata, Toshiko Kubota, and Akira Kubota for their valuable assistance in the treatment of infants admitted to the Department of Pediatrics, Chutoen General Medical Center.

Disclosures

There are no conflicts of interest to declare. This research received no specific grant from any funding agency in the public, commercial, or not-for profit sectors. Equipment of the Chutoen General Medical Center was used.

References

1. Kozák-Bárány A, Jokinen E, Kero P, Tuominen J, Rönnemaa T, Välimäki I. Impaired left ventricular diastolic function in newborn infants of mothers with pregestational or gestational diabetes with good glycemic control. *Early Hum Dev* 2004; **77:** 13–22.
2. Zielinsky P, Piccoli AL Jr. Myocardial hypertrophy and dysfunction in maternal diabetes. *Early Hum Dev* 2012; **88:** 273–278.
3. Zablah JE, Gruber D, Stoffels G, Cabezas EG, Hayes DA. Subclinical decrease in myocardial function in asymptomatic infants of diabetic mothers: A tissue Doppler study. *Pediatr Cardiol* 2017; **38:** 801–806.
4. Geyer H, Caracciolo G, Abe H, Wilansky S, Carerj S, Gentile F, et al. Assessment of myocardial mechanics using speckle tracking echocardiography: Fundamentals and clinical applications. *J Am Soc Echocardiogr* 2010; **23:** 351–369.
5. Voigt JU, Pedrizzetti G, Lysyansky P, Marwick TH, Houle H, Baumann R, et al. Definitions for a common standard for 2D speckle tracking echocardiography: Consensus document of the EACVI/ASE/Industry Task Force to standardize deformation imaging. *Eur Heart J Cardiovasc Imaging* 2015; **16:** 1–11.
6. Kalam K, Otahal P, Marwick TH. Prognostic implications of global LV dysfunction: A systematic review and meta-analysis of global longitudinal strain and ejection fraction. *Heart* 2014; **100:** 1673–1680.
7. Ishizu T, Seo Y, Enomoto Y, Sugimori H, Yamamoto M, Machino T, et al. Experimental validation of left ventricular transmural strain gradient with echocardiographic two-dimensional speckle tracking imaging. *Eur J Echocardiogr* 2010; **11:** 377–385.
8. Kobayashi M, Takahashi K, Yamada M, Yazaki K, Matsui K, Tanaka N, et al. Assessment of early diastolic intraventricular pressure gradient in the left ventricle among patients with repaired tetralogy of Fallot. *Heart Vessels* 2017; **32:** 1364–1374.
9. Popović ZB, Richards KE, Greenberg NL, Rovner A, Drinko J, Cheng Y, et al. Scaling of diastolic intraventricular pressure gradients is related to filling time duration. *Am J Physiol Heart Circ Physiol* 2006; **291:** H762–H769.
10. Yamamoto Y, Takahashi K, Takemoto Y, Kobayashi M, Itatani K, Shimizu T, et al. Evaluation of myocardial function according to early diastolic intraventricular pressure difference in fetuses. *J Am Soc Echocardiogr* 2017; **30:** 1130–1137.
11. Notomi Y, Popovic ZB, Yamada H, Wallick DW, Martin MG, Oryszak SJ, et al. Ventricular untwisting: A temporal link between left ventricular relaxation and suction. *Am J Physiol Heart Circ Physiol* 2008; **294:** H505–H513.
12. International Association of Diabetes and Pregnancy Study Groups

Consensus Panel, Metzger BE, Gabbe SG, Persson B, Buchanan TA, Catalano PA, Damm P, et al. International Association of Diabetes and Pregnancy Study Groups recommendations on the diagnosis and classification of hyperglycemia in pregnancy. *Diabetes Care* 2010; **33:** 676–682.
13. Cowie CC, Rust KF, Byrd-Holt DD, Gregg EW, Ford ES, Geiss LS, et al. Prevalence of diabetes and high risk for diabetes using A1C criteria in the U.S. population in 1988–2006. *Diabetes Care* 2010; **33:** 562–568.
14. Itabashi K, Fujimura M, Kusuda S, Tamura M, Hayashi T, Takahashi T, et al. Introduction of new gestational age-specific standards for birth size. *J Jpn Pediatr Soc* 2010; **114:** 1271–1293.
15. Yeh P, Emary E, Impey L. The relationship between umbilical cord arterial pH and serious adverse neonatal outcome: Analysis of 51,519 consecutive validated samples. *BJOG* 2012; **119:** 824–831.
16. Lang RM, Badano LP, Mor-Avi V, Afilalo J, Armstrong A, Ernande L, et al. Recommendations for cardiac chamber quantification by echocardiography in adults: An update from the American Society of Echocardiography and the European Association of Cardiovascular Imaging. *J Am Soc Echocardiogr* 2015; **28:** 1–39. e14.
17. Kenny JF, Plappert T, Doubilet P, Saltzman DH, Cartier M, Zollars L, et al. Changes in intracardiac blood flow velocities and right and left ventricular stroke volume with gestational age in the normal human fetus: A prospective Doppler echocardiographic study. *Circulation* 1986; **74:** 1208–1216.
18. Takahashi K, Nii M, Takigiku K, Toyono M, Iwashima S, Inoue N, et al. Development of suction force during early diastole from the left atrium to the left ventricle in infants, children, and adolescents. *Heart Vessels* 2019; **34:** 296–306.
19. Yotti R, Bermejo J, Antoranz JC, Desco MM, Cortina C, Rojo-Alvarez JL, et al. A noninvasive method for assessing impaired diastolic suction in patients with dilated cardiomyopathy. *Circulation* 2005; **112:** 2921–2929.
20. Greenberg NL, Vandervoort PM, Firstenberg MS, Garcia MJ, Thomas JD. Estimation of diastolic intraventricular pressure gradients by Doppler M-mode echocardiography. *Am J Physiol Heart Circ Physiol* 2001; **280:** H2507–H2515.
21. Thomas JD, Popovic ZB. Intraventricular pressure differences: A new window into cardiac function. *Circulation* 2005; **112:** 1684–1686.
22. Notomi Y, Srinath G, Shiota T, Martin-Miklovic MG, Beachler L, Howell K, et al. Maturational and adaptive modulation of left ventricular torsional biomechanics: Doppler tissue imaging observation from infancy to adulthood. *Circulation* 2006; **113:** 2534–2541.
23. Adamu U, Schmitz F, Becker M, Kelm M, Hoffmann R. Advanced speckle tracking echocardiography allowing a three-myocardial layer-specific analysis of deformation parameters. *Eur J Echocardiogr* 2009; **10:** 303–308.
24. Yamada M, Takahashi K, Kobayashi M, Yazaki K, Takayasu H, Akimoto K, et al. Mechanisms of left ventricular dysfunction assessed by layer-specific strain analysis in patients with repaired tetralogy of Fallot. *Circ J* 2017; **81:** 846–854.
25. Becker M, Ocklenburg C, Altiok E, Füting A, Balzer J, Krombach G, et al. Impact of infarct transmurality on layer-specific impairment of myocardial function: A myocardial deformation imaging study. *Eur Heart J* 2009; **30:** 1467–1476.
26. Hamada S, Schroeder J, Hoffmann R, Altiok E, Keszei A, Almalla M, et al. Prediction of outcomes in patients with chronic ischemic cardiomyopathy by layer-specific strain echocardiography: A proof of concept. *J Am Soc Echocardiogr* 2016; **29:** 412–420.
27. Yazaki K, Takahashi K, Shigemitsu S, Yamada M, Iso T, Kobayashi M, et al. In-depth insight into the mechanisms of cardiac dysfunction in patients with childhood cancer after anthracycline treatment using layer-specific strain analysis. *Circ J* 2018; **82:** 715–723.
28. Hatém MA, Zielinsky P, Hatém DM, Nicoloso LH, Manica JL, Piccoli AL, et al. Assessment of diastolic ventricular function in fetuses of diabetic mothers using tissue Doppler. *Cardiol Young* 2008; **18:** 297–302.
29. Ren Y, Zhou Q, Yan Y, Chu C, Gui Y, Li X. Characterization of fetal cardiac structure and function detected by echocardiography in women with normal pregnancy and gestational diabetes mellitus. *Prenat Diagn* 2011; **31:** 459–465.
30. Abdurrachim D, Nabben M, Hoerr V, Kuhlmann MT, Bovenkamp P, Ciapaite J, et al. Diabetic db/db mice do not develop heart failure upon pressure overload: A longitudinal in vivo PET, MRI, and MRS study on cardiac metabolic, structural, and functional adaptations. *Cardiovasc Res* 2017; **113:** 1148–1160.
31. Pibarot P, Dumesnil JG. Longitudinal myocardial shortening in aortic stenosis: Ready for prime time after 30 years of research? *Heart* 2010; **96:** 95–96.
32. Iwahashi N, Nakatani S, Kanzaki H, Hasegawa T, Abe H, Kitakaze M. Acute improvement in myocardial function assessed by myocardial strain and strain rate after aortic valve replacement for aortic stenosis. *J Am Soc Echocardiogr* 2006; **19:** 1238–1244.
33. Carasso S, Yang H, Woo A, Vannan MA, Jamorski M, Wigle ED, et al. Systolic myocardial mechanics in hypertrophic cardiomyopathy: Novel concepts and implications for clinical status. *J Am Soc Echocardiogr* 2008; **21:** 675–683.
34. Yang H, Carasso S, Woo A, Jamorski M, Nikonova A, Wigle ED, et al. Hypertrophy pattern and regional myocardial mechanics are related in septal and apical hypertrophic cardiomyopathy. *J Am Soc Echocardiogr* 2010; **23:** 1081–1089.
35. Urbano-Moral JA, Rowin EJ, Maron MS, Crean A, Pandian NG. Investigation of global and regional myocardial mechanics with 3-dimensional speckle tracking echocardiography and relations to hypertrophy and fibrosis in hypertrophic cardiomyopathy. *Circ Cardiovasc Imaging* 2014; **7:** 11–19.
36. Serri K, Reant P, Lafitte M, Berhouet M, Le Bouffos V, Roudaut R, et al. Global and regional myocardial function quantification by two-dimensional strain: Application in hypertrophic cardiomyopathy. *J Am Coll Cardiol* 2006; **47:** 1175–1181.
37. Sun JP, Stewart WJ, Yang XS, Donnell RO, Leon AR, Felner JM, et al. Differentiation of hypertrophic cardiomyopathy and cardiac amyloidosis from other causes of ventricular wall thickening by two-dimensional strain imaging echocardiography. *Am J Cardiol* 2009; **103:** 411–415.
38. Popović ZB, Kwon DH, Mishra M, Buakhamsri A, Greenberg NL, Thamilarasan M, et al. Association between regional ventricular function and myocardial fibrosis in hypertrophic cardiomyopathy assessed by speckle tracking echocardiography and delayed hyperenhancement magnetic resonance imaging. *J Am Soc Echocardiogr* 2008; **21:** 1299–1305.
39. Al-Biltagi M, Tolba OA, Rowisha MA, Mahfouz Ael-S, Elewa MA. Speckle tracking and myocardial tissue imaging in infant of diabetic mother with gestational and pregestational diabetes. *Pediatr Cardiol* 2015; **36:** 445–453.
40. Carasso S, Cohen O, Mutlak D, Adler Z, Lessick J, Aronson D, et al. Relation of myocardial mechanics in severe aortic stenosis to left ventricular ejection fraction and response to aortic valve replacement. *Am J Cardiol* 2011; **107:** 1052–1057.
41. Hein S, Arnon E, Kostin S, Schonburg M, Elsasser A, Polyakova V, et al. Progression from compensated hypertrophy to failure in the pressure-overloaded human heart: Structural deterioration and compensatory mechanisms. *Circulation* 2003; **107:** 984–991.
42. Moravsky G, Bruchal-Garbicz B, Jamorski M, Ralph-Edwards A, Gruner C, Williams L, et al. Myocardial mechanical remodeling after septal myectomy for severe obstructive hypertrophic cardiomyopathy. *J Am Soc Echocardiogr* 2013; **26:** 893–900.
43. Ingwall JS. Energy metabolism in heart failure and remodelling. *Cardiovasc Res* 2009; **81:** 412–419.
44. Pereira RO, Wende AR, Olsen C, Soto J, Rawlings T, Zhu Y, et al. Inducible overexpression of GLUT1 prevents mitochondrial dysfunction and attenuates structural remodeling in pressure overload but does not prevent left ventricular dysfunction. *J Am Heart Assoc* 2013; **2:** e000301.
45. Kolwicz SC Jr, Olson DP, Marney LC, Garcia-Menendez L, Synovec RE, Tian R. Cardiac-specific deletion of acetyl CoA carboxylase 2 prevents metabolic remodeling during pressure-overload hypertrophy. *Circ Res* 2012; **111:** 728–738.
46. Christe ME, Rodgers RL. Altered glucose and fatty acid oxidation in hearts of the spontaneously hypertensive rat. *J Mol Cell Cardiol* 1994; **26:** 1371–1375.
47. Zhong M, Alonso CE, Taegtmeyer H, Kundu BK. Quantitative PET imaging detects early metabolic remodeling in a mouse model of pressure-overload left ventricular hypertrophy in vivo. *J Nucl Med* 2013; **54:** 609–615.
48. Oakes ND, Thalen P, Aasum E, Edgley A, Larsen T, Furler SM, et al. Cardiac metabolism in mice: Tracer method developments and in vivo application revealing profound metabolic inflexibility in diabetes. *Am J Physiol Endocrinol Metab* 2006; **290:** E870–E881.
49. Lipshultz SE, Simbre VC 2nd, Hart S, Rifai N, Lipsitz SR, Reubens L, et al. Frequency of elevations in markers of cardiomyocyte damage in otherwise healthy newborns. *Am J Cardiol* 2008; **102:** 761–766.
50. Yoshibayashi M, Kamiya T, Saito Y, Nakao K, Nishioka K,

Temma S, et al. Plasma brain natriuretic peptide concentrations in healthy children from birth to adolescence: Marked and rapid increase after birth. *Eur J Endocrinol* 1995; **133:** 207–209.
51. Iwashima S, Sekii K, Ishikawa T, Itou H. Serial change in myocardial tissue Doppler imaging from fetus to neonate. *Early Hum Dev* 2013; **89:** 687–692.
52. Tyrala EE. The infant of the diabetic mother. *Obstet Gynecol Clin North Am* 1996; **23:** 221–241.
53. Okada K, Yamada S, Iwano H, Nishino H, Nakabachi M, Yokoyama S, et al. Myocardial shortening in 3 orthogonal directions and its transmural variation in patients with nonobstructive hypertrophic cardiomyopathy. *Circ J* 2015; **79:** 2471–2479.
54. Lin X, Yang P, Reece EA, Yang P. Pregestational type 2 diabetes mellitus induces cardiac hypertrophy in the murine embryo through cardiac remodeling and fibrosis. *Am J Obstet Gynecol* 2017; **217:** 216.e1–e3.
55. Iwano H, Kamimura D, Fox E, Hall M, Vlachos P, Little WC. Altered spatial distribution of the diastolic left ventricular pressure difference in heart failure. *J Am Soc Echocardiogr* 2015; **28:** 597–605.
56. Nagueh SF, Smiseth OA, Appleton CP, Byrd BF 3rd, Dokainish H, Edvardsen T, et al. Recommendations for the evaluation of left ventricular diastolic function by echocardiography: An update from the American Society of Echocardiography and the European Association of Cardiovascular Imaging. *J Am Soc Echocardiogr* 2016; **29:** 277–314.
57. Ohara T, Niebel CL, Stewart KC, Charonko JJ, Pu M, Vlachos PP, et al. Loss of adrenergic augmentation of diastolic intra-LV pressure difference in patients with diastolic dysfunction: Evaluation by color M-mode echocardiography. *JACC Cardiovasc Imaging* 2012; **5:** 861–870.
58. Yotti R, Bermejo J, Benito Y, Antoranz JC, Desco MM, Rodríguez-Pérez D, et al. Noninvasive estimation of the rate of relaxation by the analysis of intraventricular pressure gradients. *Circ Cardiovasc Imaging* 2011; **4:** 94–104.
59. Negoita M, Zolgharni M, Dadkho E, Pernigo M, Mielewczik M, Cole GD, et al. Frame rate required for speckle tracking echocardiography: A quantitative clinical study with open-source, vendor-independent software. *Int J Cardiol* 2016; **218:** 31–36.

Supplementary Files

Please find supplementary file(s);
http://dx.doi.org/10.1253/circrep.CR-19-0062